Modeling and Field-Oriented Control of the Dual Stator Winding Induction Motor in the EMTP-Type Environment

Tshibain Tshibungu

***Abstract*--The dual stator winding induction motor supplied by redundant Variable Frequency Drives (VFDs) finds its application in ship propulsion, locomotive traction, and aerospace. The redundancy of VFDs leads to reliability and safety for a continuous availability of the system even when one VFD has failed. This paper proposes the modeling in an arbitrary reference frame of dual stator winding (with an arbitrary displacement between the two three-phase winding sets) induction motor with saturation of the main flux for the EMTP-type solution. The Indirect Field Oriented Control based on the two axis d-q model of the dual stator winding induction motor is investigated and can be extended to any number of phases, which are a multiple of three. The control can be implemented using two VFDs built as an Active Front End (AFE) Rectifier followed by Voltage-Sourced Inverters (VSIs) based sinusoidal PWM or current hysteresis controller. The proposed modeling and control was simulated by using the Engineering Suite V6 software and the simulation results show the simplicity of the control scheme.**

***Keywords*: Dual Stator Induction Motor (DSIM), Indirect Field Oriented Control (IFOC), Variable Frequency Drive, AFE Rectifier.**

I. Introduction

THE concept of multiphase (more than three-phase) machine modeling and drive is not new. There are already lots of examples in literature describing multiphase machines [2]–[4], which are just a representative sample. Recently, more attention has been given to modeling and control of a multiphase motor, especially multiphase induction motors. Generally, a multiphase induction motor drive has many advantages over the conventional three-phase drive such as high power capability by dividing power between multiple phases, reduced torque pulsations and higher reliability. In particular, with the loss of one or more stator winding sets, a multiphase induction motor can continue to operate. The modeling and drive of a multiphase induction motor can use a variety of transformations. The symmetrical component theory and the matrix theory serve as theoretical foundation for these transformations. As an advantage, by segmenting equally the applied power in multiphase induction, it is possible to supply one or more windings under balanced conditions if for any reason some of them cannot be supplied. The main focus of this paper is to develop a dynamic model of the DSIM for any arbitrary angle of displacement between the two winding sets for the EMTP-type solution. The d-q model in an arbitrary reference frame model has been developed and can be used to analyze the behavior of an induction motor in any reference frame. A simple IFOC scheme control for an unsaturated DSIM is implemented using two VFDs built as Active Front End (AFE) Rectifiers followed by VSIs based hysteresis current controller. Since the DSIM is not available in standard library of most electrical software, the validation and proposed control of the Engineering Suite V6 software model (either in steady state or transient) were compared with the model built in the MATLAB/SIMULINK environment. However, only the results obtained from the Engineering Suite V6 are presented.

Tshibain Tshibungu is with Simsmart Technologies, Inc., 100-4 Place du Commerce, Brossard (Québec), Canada, J4W 3B3.

Paper submitted to the International Conference on Power Systems Transients (IPST2015) in Cavtat, Croatia June 15-18, 2015

II. Modeling of DSIM

A. Assumptions

The DSIM is designed as an electromechanical system composed on the stator side by two wye three-phase windings, which are grounded through two separate neutral impedances, referred to as stator 1 and stator 2 and on the rotor side by a common squirrel cage. The squirrel cage is replaced by an equivalent three-phase winding. The DSIM is depicted in Figure 1.

The modeling of this motor uses the following assumptions:

- Stator windings are sinusoidally distributed around the air gap,
- The two sets of stator windings are spatially shifted by an electrical angle α,
- The symmetry of the windings and only the saturation of the main flux are considered,
- The magnetic coupling between stator windings 1 and 2 is considered through the main flux; the coupling of these windings through the leakage flux is neglected,
- All the electromagnetic variables and parameters of the motor are referred to the stator side.

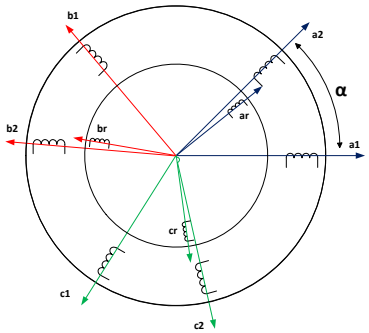

Fig. 1. Windings of DSIM

B. DSIM equations in dq0 Reference Frame

The modeling of the DSIM starts with the classical approach of modeling the three-phase induction motor. The DSIM is considered as two independent three-phase motors coupled through a common rotor winding. The Park transformations transform abc reference frame voltage and flux equations into an arbitrary dq0 reference frame. Taking into account the main flux linkage saturation by adding the d-q magnetizing flux correction terms [10] to the main flux, the voltage and flux equations into an arbitrary dq0 reference frame are as follows:

$$v_{qs1} = R_s i_{qs1} + \omega\varphi_{ds1} + \frac{d\varphi_{qs1}}{dt} \tag{1}$$

$$v_{ds1} = R_s i_{ds1} - \omega\varphi_{qs1} + \frac{d\varphi_{ds1}}{dt} \tag{2}$$

$$v_{0s1} = (R_s + 3R_n) i_{0s1} + \frac{d\varphi_{0s1}}{dt} \tag{3}$$

$$v_{qs2} = R_s i_{qs2} + \omega\varphi_{ds2} + \frac{d\varphi_{qs2}}{dt} \tag{4}$$

$$v_{ds2} = R_s i_{ds2} - \omega\varphi_{qs2} + \frac{d\varphi_{ds2}}{dt} \tag{5}$$

$$v_{0s2} = (R_s + 3R_n) i_{0s2} + \frac{d\varphi_{0s2}}{dt} \tag{6}$$

$$v_{dr} = R_r i_{dr} - (\omega - \omega_r)\varphi_{qr} + \frac{d\varphi_{dr}}{dt} \tag{7}$$

$$v_{qr} = R_r i_{qr} + (\omega - \omega_r)\varphi_{dr} + \frac{d\varphi_{qr}}{dt} \tag{8}$$

$$\varphi_{qs1} = L_{ss} i_{qs1} + L_m^{unsat} i_{qs2} + L_m^{unsat} i_{qr} + \Delta\varphi_{mq} \tag{9}$$

$$\varphi_{ds1} = L_{ss} i_{ds1} + L_m^{unsat} i_{ds2} + L_m^{unsat} i_{dr} + \Delta\varphi_{md} \tag{10}$$

$$\varphi_{0s1} = (l_{\sigma s} + 3L_n) i_{0s1} \tag{11}$$

$$\varphi_{qs2} = L_{ss} i_{qs2} + L_m^{unsat} i_{qs1} + L_m^{unsat} i_{qr} + \Delta\varphi_{mq} \tag{12}$$

$$\varphi_{ds2} = L_{ss} i_{ds2} + L_m^{unsat} i_{ds1} + L_m^{unsat} i_{dr} + \Delta\varphi_{md} \tag{13}$$

$$\varphi_{0s2} = (l_{\sigma s} + 3L_n) i_{0s2} \tag{14}$$

$$\varphi_{qr} = L_m^{unsat} i_{qs1} + L_m^{unsat} i_{qs2} + L_{rr} i_{qr} + \Delta\varphi_{mq} \tag{15}$$

$$\varphi_{dr} = L_m^{unsat} i_{ds1} + L_m^{unsat} i_{ds2} + L_{rr} i_{dr} + \Delta\varphi_{md} \tag{16}$$

Where

$\Delta\varphi_{md}, \Delta\varphi_{mq}$	d-q magnetizing flux correction terms
R_n, L_n	Neutral resistance and inductance

The mechanical equation is given as follows:

$$J\frac{d\omega_m}{dt} = T_{em} - k_d\omega_m - T_{load} \tag{17}$$

$$T_{em} = \frac{3}{2}\left(\frac{p}{2}\right)\frac{L_m}{L_{rr}}\left[\varphi_{dr}\left(i_{qs1} + i_{qs2}\right) - \varphi_{qr}\left(i_{ds1} + i_{ds2}\right)\right] \tag{18}$$

$$\omega_m = \omega_r\left(\frac{2}{p}\right) \tag{19}$$

Where

ω_m, ω_r	Mechanical and electrical speed (rad/s)
p, k_d	Number of pole and damping factor (Nm s/rad)
T_{load}, T_{em}	Load and electromagnetic torque

C. Transient Modeling

Since $v_{dr} = 0$ and $v_{qr} = 0$, equations (15) and (16) into (7) and (8) and applying the trapezoidal rule, the matrix form of rotor d-q currents in an arbitrary reference frame is as follows:

$$\begin{bmatrix} i_{dr}(t) \\ i_{qr}(t) \end{bmatrix} = [C]\begin{bmatrix} i_{ds1}(t) \\ i_{qs1}(t) \\ i_{ds2}(t) \\ i_{qs2}(t) \end{bmatrix} + \begin{bmatrix} hist_{dr}(t-\Delta T) \\ hist_{qr}(t-\Delta T) \end{bmatrix} \tag{20}$$

Where

$hist_{dr}(t-\Delta T), hist_{qr}(t-\Delta T)$	Rotor d-q history terms
ΔT	Sample time
$[C]$	2-by-4 matrix

Replacing (9) to (14) into (1) to (6) and applying the trapezoidal rule, we have:

$$\begin{bmatrix} v_{ds1}(t) \\ v_{qs1}(t) \\ v_{ds2}(t) \\ v_{qs2}(t) \end{bmatrix} = [Z]\begin{bmatrix} i_{ds1}(t) \\ i_{qs1}(t) \\ i_{ds2}(t) \\ i_{qs2}(t) \\ i_{dr}(t) \\ i_{qr}(t) \end{bmatrix} + \begin{bmatrix} hist_{ds1}(t-\Delta T) \\ hist_{qs1}(t-\Delta T) \\ hist_{ds2}(t-\Delta T) \\ hist_{qs2}(t-\Delta T) \end{bmatrix} \tag{21}$$

$$\begin{bmatrix} v_{0s1}(t) \\ v_{0s2}(t) \end{bmatrix} = \begin{bmatrix} R_{0s} & 0 \\ 0 & R_{0s} \end{bmatrix} \begin{bmatrix} i_{0s1}(t) \\ i_{0s2}(t) \end{bmatrix} + \begin{bmatrix} hist_{0s1}(t-\Delta T) \\ hist_{0s2}(t-\Delta T) \end{bmatrix} \quad (22)$$

Where

$R_{0s} = (R_s + 3R_n) + \dfrac{2(l_{\sigma s} + 3L_n)}{\Delta T}$

$[Z]$ 4-by-6 resistance matrix

$hist_i(t-\Delta T)$ Stator dq0 history terms for i = ds1, ds2, qs1, qs2,0s1,0s2

The elements in matrices $[C]$ and $[Z]$ are a function of the motor parameters and the speed deviation. Since the speed changes slowly, in comparison with the electrical quantities, and speed at time t is unknown, the equations (20) and (21) are linearized by using the predictor corrector method [8]. The following prediction is used:

$$\omega_r(t) = 2\omega_r(t-\Delta T) - \omega_r(t-2\Delta T) \quad (23)$$

The stator and rotor d-q history terms are not only dependent on previous d-q currents and speed deviation but also on previous and actual d-q magnetizing flux correction terms. Since d-q magnetizing flux correction terms at time t are unknown, the three-point predictor formula will be used (see saturation modeling).

Replacing (20) into (21), we have:

$$\begin{bmatrix} v_{ds1}(t) \\ v_{qs1}(t) \\ v_{ds2}(t) \\ v_{qs2}(t) \end{bmatrix} = \begin{bmatrix} R_{dq} \end{bmatrix} \begin{bmatrix} i_{ds1}(t) \\ i_{qs1}(t) \\ i_{ds2}(t) \\ i_{qs2}(t) \end{bmatrix} + \begin{bmatrix} e_{ds1}(t-\Delta T) \\ e_{qs1}(t-\Delta T) \\ e_{ds2}(t-\Delta T) \\ e_{qs2}(t-\Delta T) \end{bmatrix} \quad (24)$$

Where $\begin{bmatrix} R_{dq} \end{bmatrix}$ 4-by-4 resistance matrix

Applying Park's inverse transformations (see appendix), the voltage equations in abc reference frame are as follows:

$$v_{abcs1}(t) = [Z_{abcs}] i_{abcs1}(t) + [Z_{abc12}] i_{abcs2}(t) + e_{abcs1} \quad (25)$$

$$v_{abcs2}(t) = [Z_{abc21}] i_{abcs1}(t) + [Z_{abcs}] i_{abcs2}(t) + e_{abcs2} \quad (26)$$

$[Z_{abcs}]$ Self-resistance matrix

$[Z_{abcs12}], [Z_{abcs21}]$ Mutual resistance matrices

e_{abcs1}, e_{abcs2} Voltages behind resistance

D. Interfacing DSIM with EMTP-type network solution

The complete model of the DSIM for the EMTP-type solution is obtained after combining (25) and (26) in the conductance equation form as follows:

$$\begin{bmatrix} i_{abcs1}(t) \\ i_{abcs2}(t) \end{bmatrix} = [G] \begin{bmatrix} v_{abcs1}(t) \\ v_{abcs2}(t) \end{bmatrix} + \begin{bmatrix} i_{hs1}(t) \\ i_{hs2}(t) \end{bmatrix} \quad (27)$$

Where $[G] == \begin{bmatrix} [G_{abcs}] & [G_{abc12}] \\ [G_{abc21}] & [G_{abcs}] \end{bmatrix} = \begin{bmatrix} [Z_{abcs}] & [Z_{abc12}] \\ [Z_{abc21}] & [Z_{abcs}] \end{bmatrix}^{-1}$

6-by-6 conductance matrix

$\begin{bmatrix} i_{hs}(t) \end{bmatrix} = \begin{bmatrix} i_{hs1}(t) \\ i_{hs2}(t) \end{bmatrix} = [G] \begin{bmatrix} e_{abcs1}(t) \\ e_{abcs2}(t) \end{bmatrix}$ 6-by-1 current history

The modeling in a rotor, for a synchronous and stationary reference frame, are obtained respectively by setting:

$$\omega(t) = \omega_r(t), \omega(t) = \omega_s(t), \omega(t) = 0$$

Given a power system network described by the following nodal equation:

$$\begin{bmatrix} i_{hn}(t) \end{bmatrix} = \begin{bmatrix} G_n \end{bmatrix} \begin{bmatrix} v_{abcn}(t) \end{bmatrix} \quad (28)$$

Here, $\begin{bmatrix} i_{hn}(t) \end{bmatrix}$ represents the network's history current sources, $\begin{bmatrix} G_n \end{bmatrix}$ denotes the overall conductance matrix without incorporating the DSIM conductance matrix and $\begin{bmatrix} v_{abcn}(t) \end{bmatrix}$ represents the nodal voltages. A single DSIM is interfaced with the above power system network by solving (27) for the stator currents and then substituting them into (28). The final linear system of equations in terms of nodal voltages has the following standard form:

$$\begin{bmatrix} i_h(t) \end{bmatrix} = \begin{bmatrix} G_{eq} \end{bmatrix} \begin{bmatrix} v_{abcn}(t) \end{bmatrix} \quad (29)$$

Figure 2 illustrates the formulation of (29) where it is shown that $\begin{bmatrix} G_n \end{bmatrix}$ and $\begin{bmatrix} i_{hn}(t) \end{bmatrix}$ are modified by including the 6-by-6 motor equivalent conductance $[G]$ and $\begin{bmatrix} i_{hs}(t) \end{bmatrix}$ 6-by-1 motor current history terms to the corresponding motor nodes.

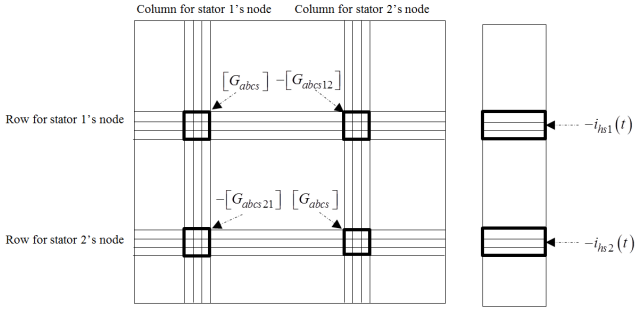

Fig. 2. Contribution of the DSIM to the network nodal equation.

E. Saturation Modeling

The characteristics of nonlinear inductance current dependent can be represented as a multi piecewise linear inductance with more slopes. Let's assume that the flux versus magnetizing current is provided (Fig. 3.), which only the first quadrant is shown, and supposed to be symmetrical.

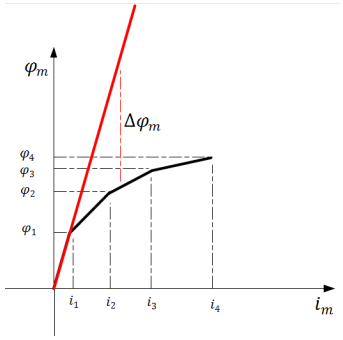

Fig. 3. Magnetizing Flux vs current of the DSIM

The magnetizing flux $\varphi_m(t)$ for a given magnetizing current $i_m(t)$ is given as follows:

$$\varphi_m^{sat}(t) = L_m^{unsat} i_m(t) + \Delta\varphi_m(t) \tag{30}$$

Where $\Delta\varphi_m(t) < 0$ is the magnetizing flux correction term.

Since the magnetizing flux versus current can be approximated as a multi piecewise linear curves as $\varphi_m^{sat}(t) = L_i i_m(t) + \varphi_i$, where φ_i is the knee point flux, the iterative algorithm for calculating the d-q flux saturation effect is as follows:

1. Calculate the magnetizing current $i_m(t)$ using the three-point predictor formula:

$$i_k(t) = \frac{5}{4} i_k(t-\Delta T) + \frac{1}{2} i_k(t-2\Delta T) - \frac{3}{4} i_k(t-3\Delta T) \tag{31}$$

$$i_{dm}(t) = i_{ds1}(t) + i_{ds2}(t) + i_{dr}(t) \tag{32}$$

$$i_{qm}(t) = i_{qs1}(t) + i_{qs2}(t) + i_{qr}(t) \tag{33}$$

$$i_m(t) = \sqrt{\left[i_{dm}(t)\right]^2 + \left[i_{qm}(t)\right]^2} \tag{34}$$

Where

i_{dm}, i_{qm} Represent d-q magnetizing current

i_k May be $i_{ds1}, i_{ds2}, i_{qs1}, i_{qs2}, i_{dr}, i_{qr}$

2. Calculate the unsaturated flux (air gap straight line), d and q mutual flux using the predicted d-q current:

$$\varphi_m^{unsat}(t) = L_m^{unsat} i_m(t) \tag{35}$$

$$\varphi_{dm}^{unsat}(t) = L_m^{unsat} i_{dm}(t) \tag{36}$$

$$\varphi_{qm}^{unsat}(t) = L_m^{unsat} i_{qm}(t) \tag{37}$$

3. Determine the appropriate piece of saturated line using $i_m(t)$ and calculate the magnetizing flux correction term:

$$\Delta\varphi_m(t) = \varphi_m^{unsat}(t) - \left[L_i i_m(t) + b_i\right] \tag{38}$$

4. Calculate d-q magnetizing flux correction terms as follows:

$$\Delta\varphi_{md}(t) = -\Delta\varphi_m(t) \frac{\varphi_{dm}^{unsat}(t)}{\varphi_m^{sat}(t)} \tag{39}$$

$$\Delta\varphi_{mq}(t) = -\Delta\varphi_m(t) \frac{\varphi_{qm}^{unsat}(t)}{\varphi_m^{sat}(t)} \tag{40}$$

III. INDIRECT FIELD ORIENTED CONTROL

Neglecting saturation and if we choose a new d-q axis rotating at a synchronous speed and aligned with the rotor field, that means $\varphi_{qr} = 0$, and the electromagnetic torque will be:

$$T_{em} = \frac{3}{2}\left(\frac{p}{2}\right)\frac{L_m}{L_{rr}} \varphi_{dr} i_{qs}^s \tag{41}$$

Where $i_{qs}^s = i_{qs1} + i_{qs2}$

If φ_{dr} is constant, which implies that $i_{dr} = 0$, the electromagnetic torque will depend only on i_{qs}^s. Hence, equations (8), (15) and (16) give:

$$\omega_s - \omega_r = \frac{R_r i_{qs}^s}{L_{rr} i_{ds}^s} \tag{42}$$

$$\varphi_{dr} = L_m i_{ds}^s \tag{43}$$

Where $i_{ds}^s = i_{ds1} + i_{ds2}$

If the magnitude φ_{dr} has to be changed, (7), (16) and knowing that $\varphi_{qr} = 0$, we have:

$$\varphi_{dr} = \frac{L_m}{1 + s\tau_r} i_{ds}^s \tag{44}$$

Where $\tau_r = \frac{L_{rr}}{R_r}$

A. VSI Based Hysteresis Current Controller

Since the inverter is controlled by a hysteresis current controller, only the speed and flux controllers should be designed.

1) Flux PI Controller Design

The following controller will output the d axis current (reference) i_{ds}^{s*}. Using (44), the open loop transfer function is given as follows:

$$T(s)=\frac{L_m k_{pf}\left(1+T_\varphi s\right)}{\left(1+\tau_r s\right)T_\varphi s} \tag{45}$$

Where

T_φ and k_{pf} are respectively the time constant and proportional gain of the flux controller.

For a given α_φ, time constant of the flux closed loop transfer function, the flux controller parameters are calculated using the Internal Model Control (IMC) and the transfer function is given as follows:

$$G_{c\varphi}(s)=\frac{\tau_r}{L_m\alpha_\varphi}+\frac{1}{L_m\alpha_\varphi s} \tag{46}$$

Since both stators must have equal d axis current, d axis current (reference) for each stator is obtained as follows:

$$i_{ds1}^{*}=i_{ds2}^{*}=\frac{i_{ds}^{s*}}{2} \tag{47}$$

2) Speed PI Controller Design

The following controller will output a reference torque T_{em}^{*}. Using (17) and (41), the open loop transfer function is given as:

$$T(s)=\frac{k_m k_{ps}\left(1+T_s s\right)}{\left(1+\tau_m s\right)T_s s} \tag{48}$$

Where

T_s and k_{ps} are respectively time constant and proportional gain of the speed controller.

$$k_t=\frac{3}{2}\left(\frac{p}{2}\right)\frac{L_m}{L_{rr}}\varphi_{dr},k_m=\frac{k_t}{k_d},\tau_m=\frac{J}{k_d}$$

By using the pole placement method, one can place poles at $s=-p_1$ and $s=-p_2$, and it will be assumed that p_1 is the dominant pole. Thus, the speed controller parameters are calculated as follows:

$$k_{ps}=\frac{\tau_m\left(p_1+p_2\right)-1}{k_m}\qquad T_s=\frac{k_m k_p}{\tau_m p_1 p_2}$$

The sum of stators q axis current is obtained by using (41), where torque and flux are respectively the outputs of speed and flux controllers. For both stators having equal q axis current, we have:

$$i_{qs1}^{*}=i_{qs2}^{*}=\frac{i_{qs}^{s*}}{2} \tag{49}$$

B. Variable Frequency Drive and Control

Figures 3, 4 and 5 summarize the implementation of the two VFDs drive DSIM. Parameters of the DSIM and load models are given in the appendix. VFDs have been designed in Engineering Suite V6 with unity power factor AFE rectifiers. DC voltage controls are based on hysteresis current controller and voltage controllers are designed using abc Reference Frame method.

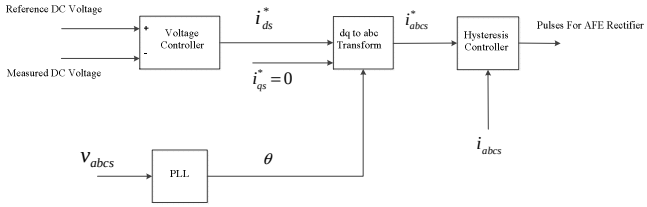

Fig. 4. Diagram block of an AFE rectifier DC voltage control

IV. Simulation Parameters

A. AFE Rectifier Controllers and Design for Unity Power Factor

Two separate 3-phase voltage sources 460 V, 60 Hz, $R_s=0.15\ \Omega, L_s=8$ mH supply two AFE rectifiers that feed the inverters. The DC reference voltage is set to 1000 Volts. The IGBT (modeled by ideal switch in parallel with a diode) is triggered by a hysteresis control which is set to $h=\pm 0.1$ A. The diode snubber RC are $C_{sn}=0.1\ \mu$F and $R_{sn}=500\ \Omega$. The capacitor is initially charged at 1000 Volts and $C=5000\ \mu$F.

TABLE I
AFE RECTIFIER VOLTAGE CONTROLLER PARAMETER

	k_{pv}	k_{iv}
Voltage controller	0.32	15.45

Where

k_{pv} and k_{iv} are respectively the proportional and integral of the rectifier voltage controller.

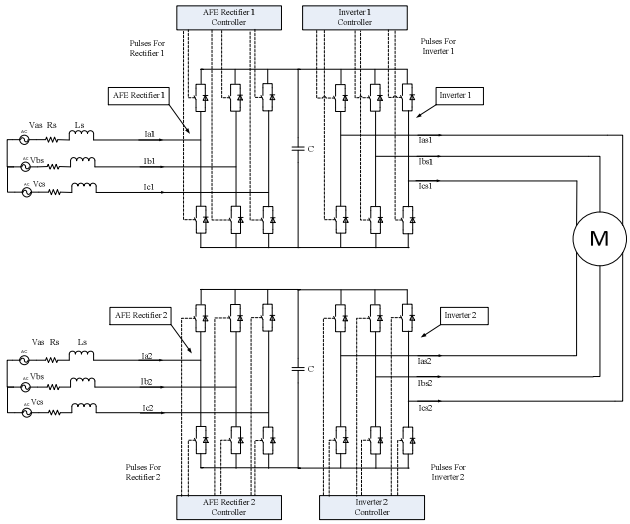

Fig. 5. Diagram of VFDs drive DSIM

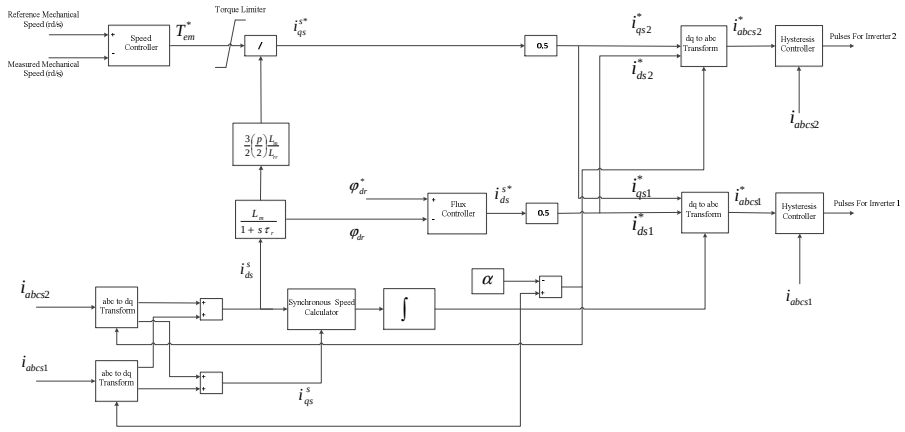

Fig. 6. Diagram block of the DSIM speed control with IFOC

B. DSIM Controllers and Design

The two inverters that control the DSIM are controlled by a hysteresis current controller. The hysteresis control is set to h = ± 0.5 A . Using the formulas developed for speed and flux controllers, the following table summarizes the PI Controllers parameters.

TABLE II
DSIM FLUX AND SPEED CONTROLLER PARAMETERS

	k_p	k_i
Flux controller	449.57	2881.884
Speed controller	23.54	107

Where

k_p and k_i are respectively the proportional and integral of the flux or speed controller.

V. SIMULATION RESULTS

The first scenario was carried out to compare online start-up of the saturated (black color) and unsaturated (blue color) motor driving load model 1. Figures 7 and 8 show the speed (rad/s) and electromagnetic torque (Nm) of the saturated and unsaturated motor using the model implemented in the Engineering Suite V6. Figures 9 and 10 show the stator currents (A) of both stators (case of unsaturated motor).

The second scenario was carried out using VFDs to drive the DSIM connected to the load model 2. A reference speed of 120 rad/s and -120 rad/s are applied respectively at t = 0 s and t = 1.6 s. Figures 11 and 12 show control of electromagnetic torque and speed. Torque is limited to 500 Nm as requested. Figures 13 and 14 show transient and steady state of both stator currents (A). Both currents are equal in magnitude since d-q current controls are equally shared between both stators. Figure 15 shows control of the flux (Wb) versus its reference.

The third scenario studies the behavior of losing one of the inverters when the system is connected to load model 2. A reference speed of 120 rad/s is applied and inverter 2 is lost at t = 1.4 s. Figures 16 and 17 show speed (rad/s) and electromagnetic torque (Nm). As expected at t = 1.4 s when inverter 2 is disconnected, speed and torque drop. The torque falls to half of the steady state value before increasing to the desired value requested by the speed controller in order to

meet the reference speed. As a consequence, Figures 18 and 19 show transient and steady states of both stator currents (A), where stator 1 current is double the steady state value. Figure 20 shows the transient of flux (Wb).

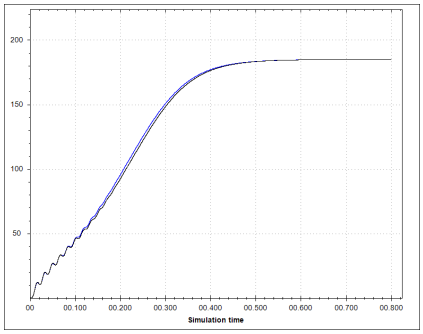

Fig. 7. Speed for unsaturated vs saturated motor

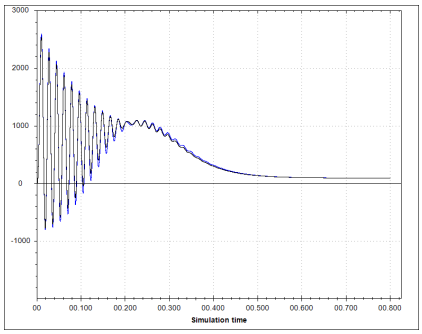

Fig. 8. Torque for unsaturated vs saturated motor

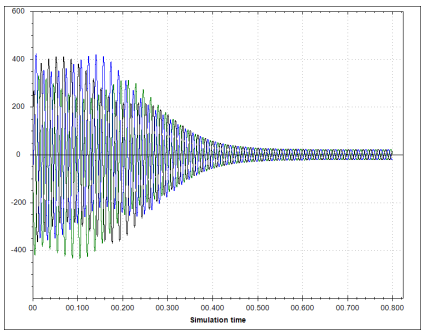

Fig. 9. Stator 1 current for unsaturated motor

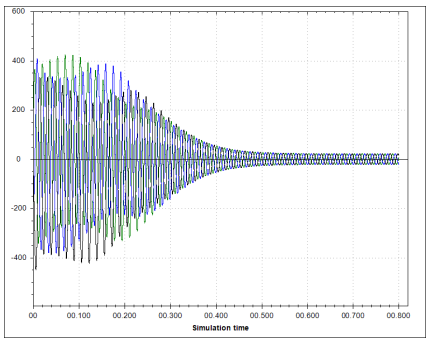

Fig. 10. Stator 2 current for unsaturated motor

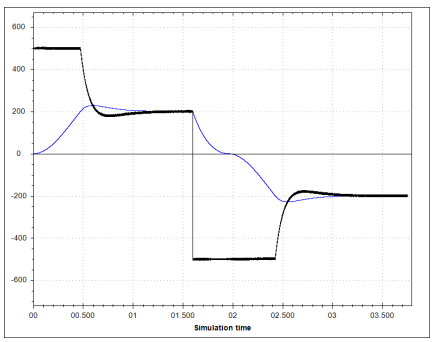

Fig. 11. Electromagnetic vs Load torque

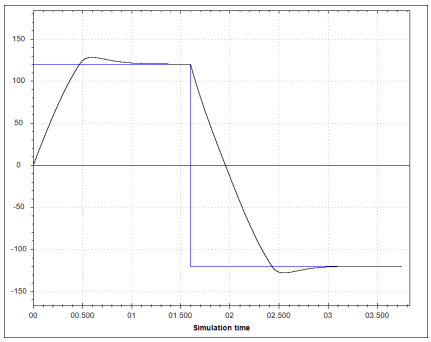

Fig. 12. Speed vs reference

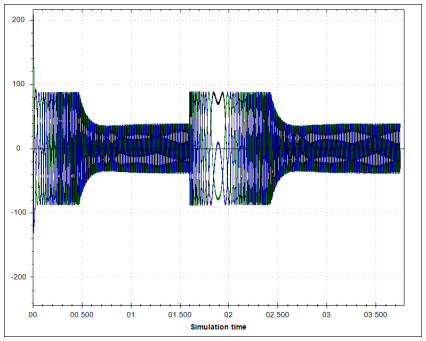

Fig. 13. Transient-DSIM stator 1 current

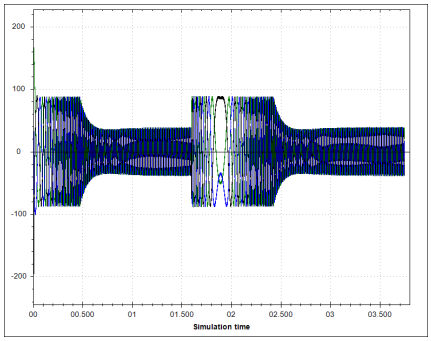

Fig. 14. Transient-DSIM stator 2 current

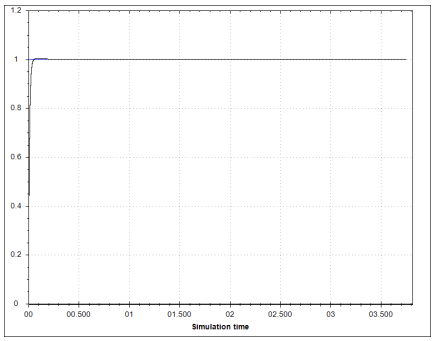

Fig. 15. Magnetizing flux vs reference

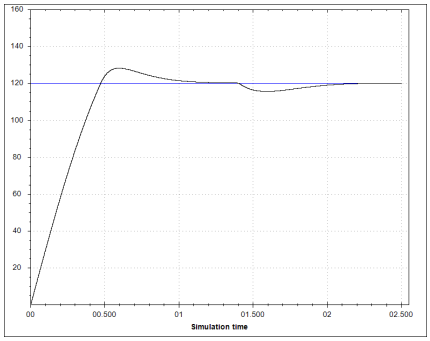

Fig. 16. Speed vs reference

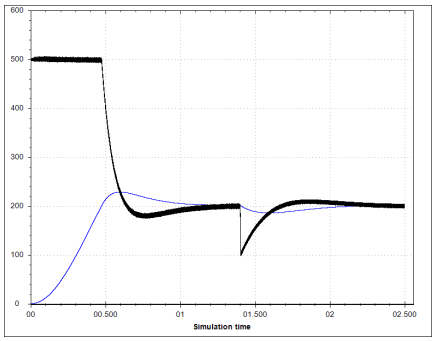

Fig. 17. Electromagnetic vs Load torque

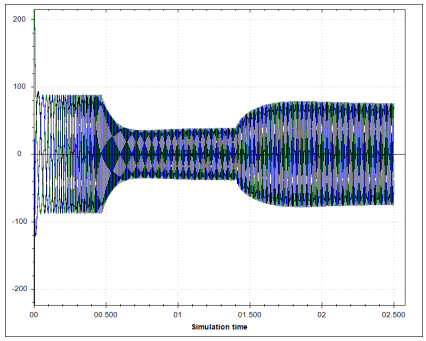

Fig. 18. Transient-DSIM stator 1 current

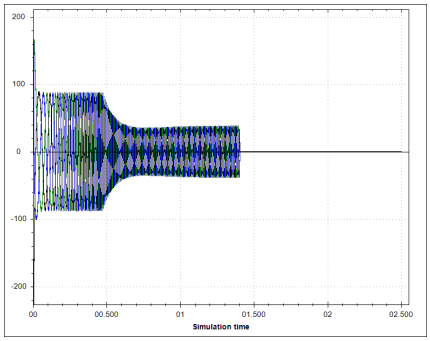

Fig. 19. Transient-DSIM stator 2 current

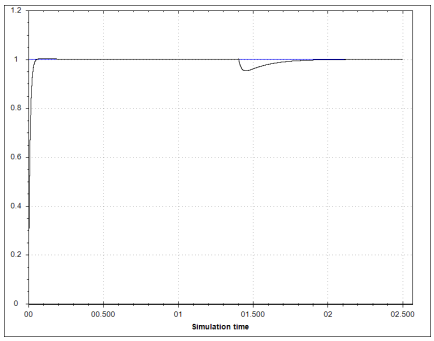

Fig. 20. Magnetizing flux vs reference

VI. Conclusions

The modeling of the DSIM for the EMTP-type solution and a simple approach to the IFOC has been presented. The validity of the model and control was verified by several informative simulations. The modeling and control of the DSIM are based on a two axes d-q model, and can be easily extended to any number of phases, which are a multiple of three. The DSIM can be modeled in any reference frame and any arbitrary angle displacement between the two three-phase winding sets.

The redundancy of the VFDs improves reliability and availability of the system even when one VFD has failed. Within the acceptable limit for the DSIM current, the simple IFOC presented allows control of the DSIM under balanced conditions and required torque even when one of the inverters is out of service.

VII. Appendix

The DSIM is a 460 V, 60 Hz, 4 poles and $\alpha = 30^0$. The maximum torque allows is 500 Nm and the motor is ungrounded through an impedance $R_n = 1e5\,\Omega,\ L_n = 0\,mH$.

The DSIM parameters are given in table III.

TABLE III
DSIM PARAMETERS

Stator resistance	R_s	$0.087\,\Omega$
Rotor resistance	R_r	$0.228\,\Omega$
Rotor leakage inductance	$l_{\sigma r}$	$0.8\,mH$
Stator leakage inductance	$l_{\sigma s}$	$0.8\,mH$
Magnetizing inductance	L_m	$34.7\,mH$
Moment of Inertia	J	$1.662\,kgm^2$
Rated flux	φ_{dr}^*	$1Wb$

Saturation curve

$$\varphi_m = \begin{cases} 0.0347 i_m & (Wb) \quad For\ i_m \le 28.9A \\ 0.801 + 0.0069 i_m & (Wb) \quad For\ i_m > 28.9A \end{cases}$$

Load Models

$$T_{load1} = 0.5\omega_m, T_{load\,2} = sign(\omega_m) * 0.0139\omega_m^2$$

Park's inverse transformations

$$[f_{abc}] = \begin{bmatrix} sin\gamma & cos\gamma & 1 \\ \sin(\gamma - 2\pi/3) & \cos(\gamma - 2\pi/3) & 1 \\ \sin(\gamma + 2\pi/3) & \cos(\gamma + 2\pi/3) & 1 \end{bmatrix} [f_{dq0}]$$

Where

For the rotor $\gamma = \theta - \theta_r$, for the stator 1 $\gamma = \theta$ and the stator 2 $\gamma = \theta - \alpha$.

f : Voltage or current

θ_r: Angle between stator and rotor identical phase

θ: Angle between q axis and stator phase A

VIII. References

[1] Alf Kare Adnames, "Maritime Electrical Installations and Diesel Electric Propulsion," ABB AS Marine, Oslo, April 2003.

[2] Singh G. K., Nam K. and Lim S. K., "A simple indirect field-oriented control scheme for multiphase induction motor," *IEEE Trans. Ind. Elec.*, vol.52, Aug. 2005.

[3] A. Munoz and T. A. Lipo, "Dual stator winding induction machine drive," *IEEE Trans. Ind. Appl.*, vol.36, Sept/Oct. 2000.

[4] T. A. Lipo, "A d-q model for six phase induction machines," Proc. Int. Conf. Electric Machines, Athens, Greece, 1980.

[5] D. W. Novotny and T. A. Lipo, *Vector Control and Dynamics of AC Drives.* Oxford, U.K. Clarendon, 1996.

[6] Zhao Y. and T. A. Lipo, "Space Vector PWM Control of Dual Three-Phase Induction Machine Using Vector Space Decomposition," *IEEE Trans. Ind. Appl.*, vol.31, 1995.

[7] G.K. Singh, "Multi-phase induction machine drive research- A survey," Elect. Power Syst. Res., vol. 62, 2002.

[8] Dommel, H. W., *EMTP Theory book*, Microtran Power System Analysis Corporation, Vancouver, 1996.

[9] Hubert Razik, *Handbook of Asynchronous Machines with Variable Speed.* 1st Edition, Wiley, 2011.

[10] P. C. Krause, O. Wasynczuk, S.D. Sudhoff, *Analysis of Electric Machinery and Drive Systems.* 2nd Edition, IEEE Press, Wiley-Interscience, 2002.

[11] M. P. Kazmierkowski, F. Blaabjerg, R. Krishnan, *Control In Power Electronics. Selected Problems.* Academic Press, 2002.

[12] Graham C. Goodwin, Stefan F. Graebe, Mario E. Salgado, *Control System Design.* 1st Edition, Prentice Hall, 2000.